To Study the Fluid-Structure Interaction (FSI) Phenomenon of Non-Newtonian Viscoelastic Fluid

Chirag Chauhan[1], Somvir Arya[2]

[1]Research Scholar, Mechanical Engineering Department, Indus Institute of Engineering & Technology, Kinana (Jind) Haryana India
[2]Assistant Professor & Head, Mechanical Engineering Department, Indus Institute of Engineering & Technology, Kinana (Jind) Haryana India

---

Abstract: *It is well known that when a flexible or flexibly-mounted structure is placed perpendicular to the flow of a Newtonian fluid, it can oscillate due to the shedding of separated vortices at high Reynolds numbers, if the same flexible objects are placed in non-Newtonian flows; however the structure's response is still unknown. The main objective of the work is introduce a new field of viscoelastic fluid-structure interactions by showing that the elastic instabilities that occur in the flow of viscoelastic fluids can drive the motion of a flexible structure placed in its path. Unlike Newtonian fluids, the flow of viscoelastic fluids can become unstable at infinitesimal Reynolds numbers due to the onset of purity elastic flow instability. This instability occurs in the absence of nonlinear effects of fluid inertia and Reynolds number of the flows studied here are in the order of 10-04. When such elastic flow instability occurs in the vicinity of a flexible structure, the fluctuating fluid forces exerted on the structure grow large enough to cause a structural instability which in turn feeds back into the fluid resulting in flow instability. Nonlinear periodic oscillations of the flexible structure are observed which have been found to be coupled to the time-dependent growth and delay of viscoelastic stresses in the wake of the structure. Presented in this work are the results of an investigation of the interaction occurring in the flow of a viscoelastic wormlike micelle solution past a flexible rectangular sheet. The structural geometries studies include: flexible sheet inclination at 20°, 45°, 90° and flexible sheet width of 5mm and 2.5mm. By varying the flow velocity the response of the flexible sheet has been characterised in terms of amplitude and frequency of oscillations. Steady and dynamic shear theology and filament stretching extensional rheology measurement are conducted in order to characterize the viscoelastic worm like micelle solution. Bright field image show the deformation of the flexible sheet during an unstable oscillation while flow-induced birefringence images highlight the viscoelastic fluid stresses produced in the wake of the flexible sheet.*

Keywords: Fluid, FSI, Newtonian, Non-Newtonian, Viscoelastic

1. Introduction:

1.1 Non-Newtonian fluids:

Non-Newtonian fluid are a significant component in daily life showing many interesting characteristics, the most important being that may behave like an elastic. These fluids are often called viscoelastic fluids. The combination of viscosity and elasticity is imparted by the physical nature of the macromolecules in these fluids, which may be present in the form of high molecular weight polymers, self-assembled wormlike micelle stretches within a flow field, it is deformed out of its equilibrium random configuration. An elastic restoring force results, driving the polymer or micelle back towards its entropically favourable equilibrium state [1]. This leads to a characteristic fluid timescale known as the relaxation time,

$$\lambda=\frac{\eta}{G} \qquad (1)$$

which describe the time required for the polymer coil or wormlike micelle to relax from a deformed state back to its equilibrium configuration. Here η is the viscosity and G is the elastic modulus of the fluid. For these fluids, Newton's law of viscosity no longer holds. They are therefore describing as non-Newtonian fluids. Thus, the residence time of a fluid in a flow must also be considering to understand the viscoelastic fluid's response. The relative importance of elasticity in a flow is described by a Deborah number which is the ration of the relaxation time of the fluid to a characteristic deformation timescale,

$$De=\frac{\lambda}{t} \qquad (2)$$

2. Literature:

If the deformation timescale is large in comparison to the relaxation time of the fluid, De<1, then the polymer coil has ample time to relax back to equilibrium and the fluid will behave like a Newtonian fluid. If the relaxation time is much longer than the deformation timescale in the flow, De>1 then the fluid will react like an elastic Hookean solid. The behaviour of the fluid between these two extremes is quite rich. Viscoelastic worm like micelle solutions are currently

being used extensively as rheological modifiers in consumer products such as paints, detergents, pharmaceuticals, lubricants and emulsifiers where careful control of the fluid properties are required. In addition, micelle solutions have also become important in a wide range of applications including agrochemical spraying, inkjet printing, and turbulent drag reduction and enhanced oil recovery where they are often used as a polymer-free fraction fluid for stimulating oil production [2-4]. A fundamental understanding of the behaviour of these complex fluids in different flow regimes is therefore extremely important to a host of industries. Techniques for the analysis and control of the flow of complex fluids require accurate determinate of the material properties as well as the ability to understand and predict changes that occur within the materials as they are subjected to the flow conditions encounter in industrial and commercial applications. Shear and extensional rheometers provide an excellent framework for investing the behaviour of these complex flows and phenomena such as elastic flow instabilities, which commonly occur in many of the industrial and commercial applications mentioned above. A number of studies of the nonlinear rheology and the behaviour of these complex fluids in strong flows have recently been published. Surfactants are amphiphilic molecules which have both a bulky hydrophilic head, which is often charged, and a relatively short and slender hydrophobic tail typically consisting of an 8-20 carbon atom chain. Above their critical micelle concentration (CMC), surfactant molecules in water will spontaneously self-assemble into large aggregates knows as micelles are formed where instead the head- groups are shield from the oil [5-7]. In oil, reverse micelle are formed where instead the head-groups are shielded from the oil [8-9]. As seen in figure 1.1, these large aggregates can form into a number different complex shapes including spherical and wormlike micelle, vesicles and lipid bilayers [10]. The morphology of the aggregates depends on the size of the surfactant, the salinity of the solution, temperature and the flow conditions [5,10]. We are most interested in wormlike micelle display many of the same viscoelastic properties of polymers. However, although both wormlike micelle solutions and polymers can be viscoelastic, wormlike micelle are physically quite different from polymers. Whereas the backbone of a polymer is covalently bonded and rigid, wormlike micelle are held together by relatively-weak physical attractions and as a result are continuously breaking and reforming with time. In an entangled network, both individual polymer chain and wormlike micelle can relieve stress through reputation driven by Brownian motion [6]. However, unlike polymeric fluids, wormlike micelle solutions have access to a number of stress relief mechanisms in addition to reputation. Wormlike micelle can relieve stress and eliminate entanglement points by either breaking and reforming in a lower stress state [7] or alternatively by creating a temporary branch point which allows two entangled micelles to pull right through each other thereby eliminating the entanglement point and relieving stress in what has become known as " ghost-like" crossing[11]. Additionally, the constant re-organisation of the network structure results in several interesting phenomenon when subjected to strong flows. Under all but, the most extreme conditions, these solutions large viscoelastic lead to a vanishingly small Reynolds number,

$$\mathrm{Re} = \frac{\rho V L}{\mu} \qquad (3)$$

Where ρ is the fluid density, U is the flow velocity, L is the characteristic length scale and μ is the fluid viscosity. In all of the experiments presented in this work, the Reynolds number is of order $10^{-}4$. An interesting feature of wormlike micelle is their mechanism of mechanical failure under as applied stress. Flow curves have shown these solutions to be shear thinning [7], and strain hardening [12], however these two non-Newtonian behaviour do not predict their method of failure. In extensional flow, when a fluid filament experiences a large enough stress, the value of which is independent of strain rate it falls dramatically at its mid plane. This behaviour has been observed most recently by Rothstein et al. [13], and is believed to be caused by a scission of individual micelle chains. This type of dramatic failure can manifest itself as instabilities in not just extensional flows, but complex flows as well. For example, the flow around a sphere contains regions of shear as the fluid passes around the circumference, as well as extension in the wake of the sphere. Given that the fluid is known to be shear thinning as well as extensionally thickening, the combination of these qualities and the complex flow field yields some interesting results. Chen and Rothstein [14] observed that above a critical Deborah number a new class of elastic instabilities, related to the rupture of these micellar solutions in the extensional flow Present in the wake of a sphere occurred. By measuring the flow fields with PIV and FIB they were able to explore the kinematics of the flow. Similar instabilities have also been observed by Belmonte et al. [15].

VIV of a flexibly-mounted rigid cylinder with a circular cross-section placed in fluid flow and free to oscillate in the cross-flow direction i.e. the direction perpendicular to the oncoming flow, has become the canonical problem in FSI. Work by several investigators has helped elucidate the fundamental of VIV [16, 21-27].

2.1 Objective

The goal of this work is to study fluid-structure interaction (FSI) phenomena in which the fluid is a non-Newtonian viscoelastic fluid and the structure is flexible. FSI has been studied extensively for structures in contact with Newtonian fluid where the shedding of separated vortices at high Reynolds numbers can drive the motion of a flexibly- mounted or flexible structure. There are, however, no studies in the literature of FSI for viscoelastic fluids. Unlike Newtonian fluids, the flow of viscoelastic fluids can become unstable even at very small Reynolds members in the order of $10^{-}4$ seen in literature for flow past stationary objects. This flow instability can provide a periodic driving force on flexible structures, resulting in

a new class of FSI problems. This phenomenon has not been studied. FSI of viscoelastic fluid is an open problem with the potential to have a transformative impact on the field of fluid-structure interactions. In our study, we have observed structural instabilities caused by instabilities of a non-Newtonian viscoelastic fluid.

A large body of work exists on low Reynolds number swimmers. In the case of swimming, a two way coupling between flow and structure is not needed: the structure pushes the fluid around it in order to propel itself. A number of recent numerical and experimental studies have been investigated the importance of viscoelasticity on the propulsion of different model micro-organism. The two ways coupling between the viscoelastic fluid instability and structural instability is the focus of the work.

3. Experimental Setup:

A flexible natural rubber sheet having a length of 50mm, width 5mm and thickness 0.3mm served as the deformable structure. The flexible sheet was clamped at both ends to the walls at the midplane of the rectangular channel and aligned perpendicular to the flow direction. The flexible sheet had an elastic modulus of E =101 kPa and its natural frequency was measured to be fn = 0.15 Hz from pluck Tests of the mounted sheet in air. This measurement closely matches the predictions for a beam with clamped ends The flow cell was made of anylic· so it would be transparent and had an internal cross section of 50 mm **x** 50mm and a length of 450 mm. In order to avoid containment effects. The flexible sheet was placed such that a sheet to channel width of at least 5: 1 can be maintained. In this way, the greatest shear gradient experienced by the test fluid will be along the flexible sheet and not the bounding channel walls. Extensional rheology of this solution has been discussed in the fluid rheology section. To minimize the driving pressure fluctuations, a positive displacement piston pump was fabricated and used to produce a precisely controllable, constant flow rate through the channel.

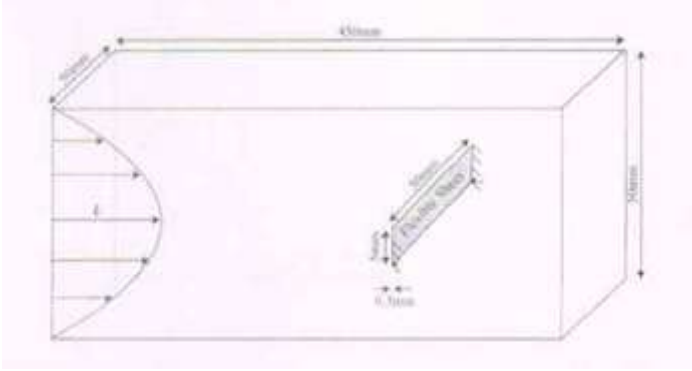

Figure: 1 Schematic diagram of the geometry used to study the flow of wormlike micelle solution past a flexible sheet

The piston motion was controlled with addressable micro-staging, capable of a flow rate resolution of $4mm^3/s$. Due to the precision of the pumping system. The flow velocity can be accurately controlled, allowing for a repeat-able and accurate interrogation of the test. In the study, the flow velocity was varied from 0 to 14mm/s to explore the flexible sheet deforination. fluid-structure interaction and flow induced birefringence as a function of the average flow velocity.

3.1 Structural deformation tracking

In order to quantitatively measure the deformation of the flexible sheet during the flow of the test fluid, discrete points were marked along the length of the sheet as showing Fig. 2. Duriug the test, the motion of the flexible sheet was captured using a high speed camera (Phantom V 4.2). Using a high speed camera allowed videos to be recorded at 100 frames per second. The captured high resolution video were then used *as* an input in a tracking software (Tracker), which located and tracked the motion of discrete points and provided the displacement time histories a teach point for each frame.

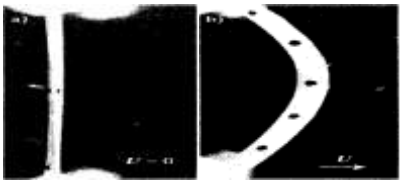

Figure 2. Flexible sheet position at (a) rest and (b) under flow conditions.

From zero to a specific flow velocity, where in the flexible sheet deformed from the no-How position to a deformation having a static displacement. In the experiments conducted for this study, the flexible sheet showed

only the first mode of excitation in the unstable oscillations. Therefore, only the midsection point on the sheet was input the tracking software and this was sufficient to gain information regarding the amplitude and frequency of oscillations. For each time history, a minimum of 180 seconds of data was collected once the flexible sheet achieved at steady mean displacement. Additionally, in order to illustrate the complex deformation under gone by the flexible sheet for each cycle of oscillation. Bright field images were captured using a Nikon D70 digital camera at small time increments within a single oscillation cycle for various flow velocities These sets of image were critical in determining the total stress experienced by the flexible sheet based on the total deformation of the sheet profile visible in the bright field image:-;. This total stress was in fact applied by the viscoelastic fluid flowing past the flexible sheet. Thus, the bright. Field images helped in relating the deformation of the flexible sheet with the stresses developed in the viscoelastic fluid.

4. Result & Discussion:

A series of measurements were made over a range of flow velocities where the maximum Reynolds number of *Re* =3.5x10-was attained. Reynolds number is defined as, $Re=\mu Uw/r70$ where μ is the density of the fluid, *U* is the flow velocity, *W* is the width of the sheet, and 170 is the zero shear rate viscosity. The *Ire* signifies the strength of inertial effects in a flow. As *Re* is very small, these experiments are in the Stokes flow regime and the interial flow effects can be neglected. At zero flow velocity. The sheet is undisturbed and aligned perpendicular to C' flow direction seen in Fig. 3. As the cross flow applied, the sheet is bent in the flow direction. Here we observe that in addition to the induced curvature along the length of these l wet that can be observed from the front. View in Fig. 3, the low flexural rigidity of the sheet results in a secondary curvature across the sheet that can be observed from the side view in Fig. 3. The resulting cross-sectional profile is 'c· shaped. At low flow velocities, where the Weissenberg number **in** small, the How of the worm like micelle solution remains stable and, as seen in Fig. 3. the static deflection of the sheet grows within creasing average flow speed. As the flow velocity is increased beyond a critical velocity and a corresponding critical weissenberg number. The flow of the wormlike micelle solution becomes unstable and this in turn affects the stability of the flexible sheet displacement. At this stage, the flexible sheet does not have a constant displacement, but rather begins to oscillate about its stretched position. As was the case for the flow of wormlike micelle solutions past circular cylinders and spheres [14], the flow instability originates as low growth and fast decay of extensional stress in the wake of the flexible sheet. The bifurcation diagram of Fig. 3 shows the maximum and minimum deformations of the flexible sheet versus flow velocity. Below *Ucrit* =1.43mm/s, the flow is stable and the structure under goes a static deflection but does not oscillate. The *Wi* at this point corresponds to

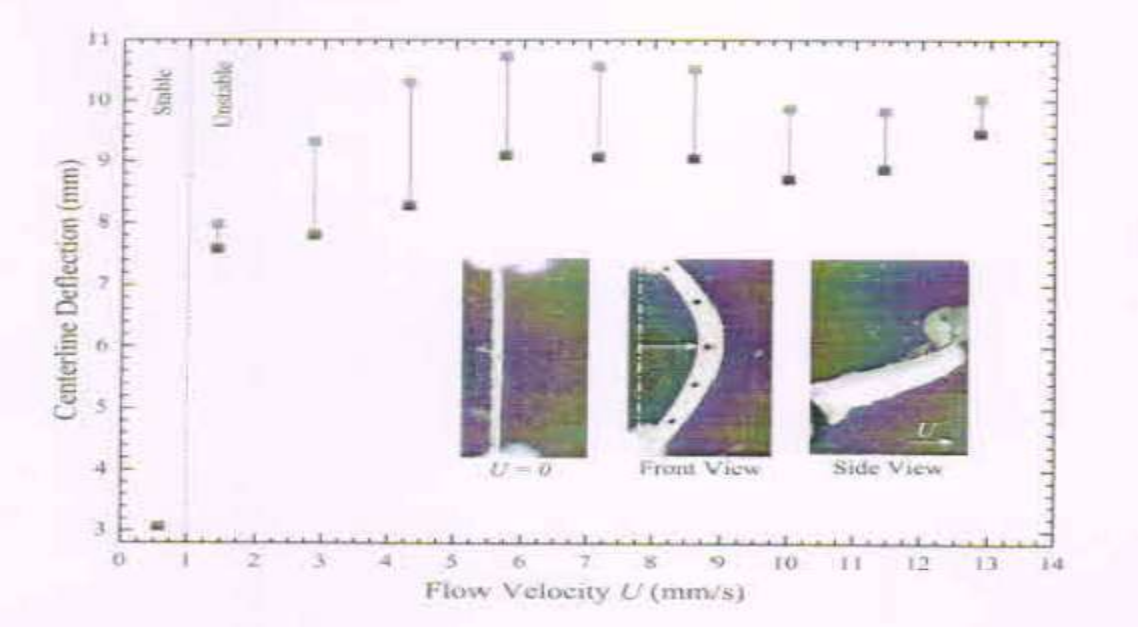

Figure: 3 Bifurcation diagram of the ceut.er line deflection of the flexible sheet versus the flow velocity

spheres [14,54], the flow instability originates as low growth and fast decay of extensional stress in the wake of the flexible sheet. The bifurcation diagram of Fig. 3 shows the maximum and minimum deformations of the flexible sheet versus flow velocity. Below *Ucrit* =1.43mm/s, the flow is stable and the structure under goes a static deflection but does not oscillate. The *Wi* at this point corresponds to.

$$Wi_{crit} = \lambda \frac{U_{crit}}{H} = 47s \frac{1.43mm/s}{5mm} = 13.4$$

Above *Ucrit* ,a periodic response is observed. Just beyond the bifurcation point, the maximum displacement of the flexible sheet increases linearly with flow velocity until a velocity of *U* =6mm/s. beyond which, the maximum sheet deflection reaches a plateau and remains more or less unchanged for all flow velocities tested. On the Other hand, the amplitude of the sheet oscillations increases linearly untilit reaches a maximum at *U*=4mm/s.There after, with increasing flow velocity, the oscillation amplitude decays.

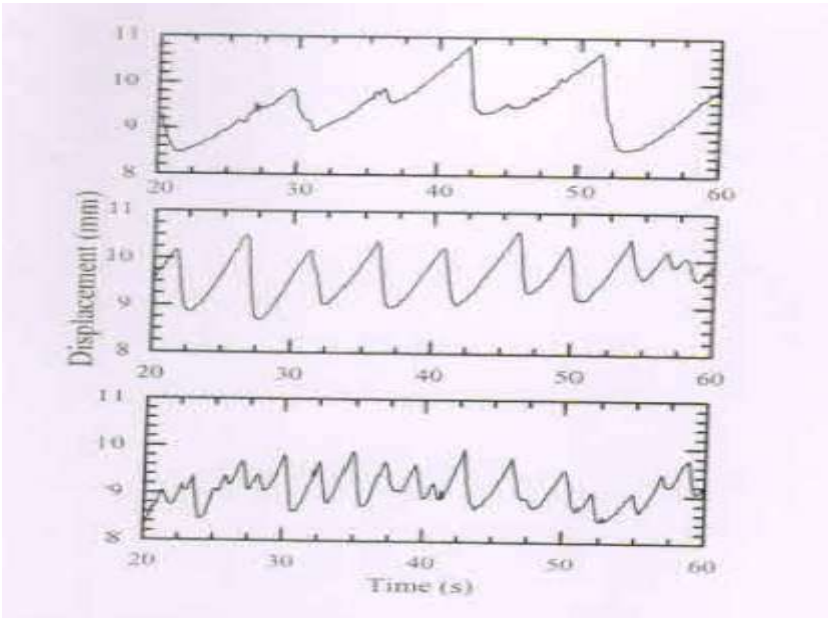

Figure: 4 Time histories of the center line deflection of the flexible sheet at (a) *U* =4.3mm/s. (b) *U*=7.15mm/s, and (c)*U*=11.44mm/s

The time histories of these oscillations at specific flow rates have been presented in Fig.4. At *U*=4.3mm/s, where the structure has begun to oscillate. The flexible sheet stretches slowly with the slope at. 0.17mm/s untila failure in the elastic fluid stresses in its wake because the flexible sheet to recoil a bruptlyaad the decay slope is considerably quicker at 2mm/s. As the flow rate is increased. The oscillations of the flexible sheet increases in frequency with its stretching rate increasing to U.47mm/s at *U*=7.15mm/s The rate at which the flexible sheet recoils continues to beat 2mm/s. With increased flow rates, the oscillations of the flexible sheet continue to become More repetitive and it has a faster stretching rate of 0.68mm/s at *U*=11.44mm/s.

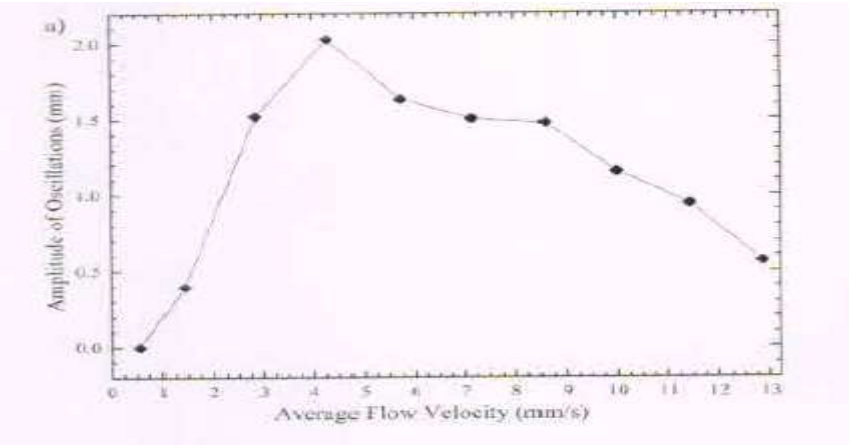

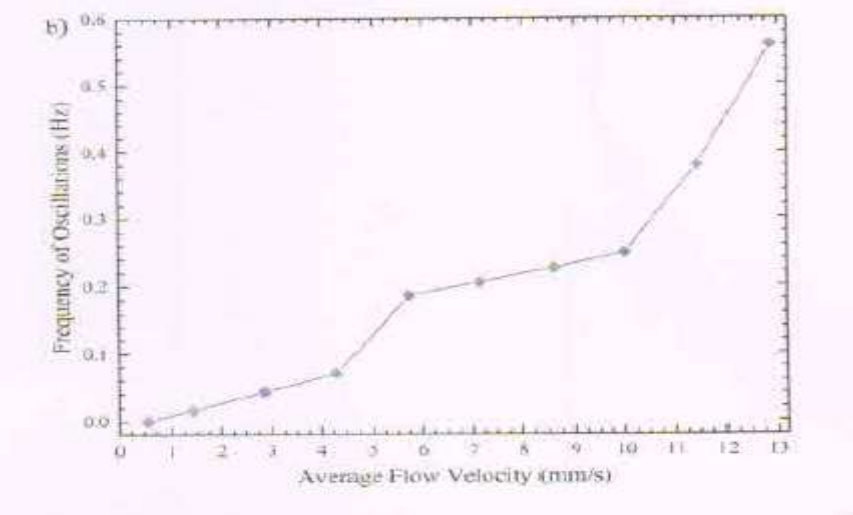

Figure: 5 The (a) amplitude and (b) frequency of the flexible sheet oscillations plotted as a function of the flow velocity

The recoil rate of the flexible sheet stays the same. The oscillations of the flexible sheet at this flow rate and beyond become very chaotic and seem to show higher harmonics. Another important observation from the time history plots of the flexible sheet is the smoothness of the displacement curve. At the lower flow rate of 4.3mm/s, the stretching of the flexible sheet is not uniform. There are minor peaks 011 the way of reaching the maximum displacement point in the oscillation cycle. How rate increasing to 7.15mm/s, the stretching of the sheet is smooth and the time history curve is a well-defined saw-tooth pattern. The higher frequency oscillations occurring at flow rates of 10mm/s and beyond. Show a non-uniform pattern of peaks with no definite minimum and maximum displacement point in oscillation cycles. At low flow velocities, the sheet is able to fully recoil before any significant extensional stress can be rebuilt in the wake. This results in a smooth deflection of the flexible sheet with sudden and dramatic recoil of the sheet leading up to maximum amplitude. The deformation rate of the flexible sheet also increases and becomes comparable to the recoil rate of the sheet. At this point the flexible sheet does not achieve complete recoil since the recoil rate is Hot faster than the growth of extensional stresses in the wake of the flexible sheet anymore. As a result, the amplitude of oscillations can be observed to decay with increasing flow velocity. Secondly, once the flow velocity gets beyond *Ucrit,* the rapid recoil of the flexible sheet is found to occur due to a centralized break down of extensional stress in the wake of the sheet. However, this phenomenon does not stay the same at higher flow velocities. As a result, local breakdowns in the fluid extensional stress at various regions along the span of the flexible sheet begin to dominate which effectively decrease amplitude of oscillations while increasing the frequency as seen in Fig. 5

Figure: 6 The bright and dark regions in the wake of the flexible sheet in the images seen above highlight the different states of extensional fluid stresses. In (a), at a lower flow velocity U=7.3mm/s. the stresses developed are uniform as seen by the uniformly dark area in the image. At a higher flow velocity shown in (b) and (c), the extensional stresses are not uniforms seen by their regular bright and dark regions along the span in the wake of the flexible sheet

5. Conclusion:

In this work, the results of an investigation into the existence of non-Newtonian fluid-structure interactions are presented Fluid-structure interaction studies have until now only comprised of Newtonian fluids used as test fluids. In this study, we show that the elastic instabilities occurring during the flow of non-Newtonian fluid scan also drive the motion of structure resulting in a new and as yet unexplored field of FSI studies. By systematically varying the flow velocity, flow kinematics, flexible sheet displacement and bifurcation diagram were obtained and used to characterize viscoelastic fluid- structure interactions.

REFERENCES:

[l] P. Flory. *Principles of Poly1mer Chemistry.* Ithaca: Cornell University Press,1953

[2] V. Anderson, J. Pearson, and E. Book, the rheology of worm-like micellar fluids. In *Rheology Reviews ,* D. Binding and K Walters, Eds. The British Society of Rheology, 2006, vol. 4,pp.217-253.

[3] S. kefi. J. Lee, T. Pope. P. Sullivan..E. Nelson, A. Hernandez, T. Olsen, M. Parlar, B. Powers, A. Roy, A. Wilson. and A. Twynam, "Expanding applications for viscoelastic surfactants," *Oilfield Review.* pp. 10-16, 2004.

[4] J. Zakin and H. Bewersdorff. "Surfactant drag reduction," *Rev .Chem. Eng.,* vol.14,no.45,pp.253--320, 1998.

[5] J. N. Israelachvili, *Interrnolecular and surface forces :with applications to col-loidal and biologicalsystems.*London:AcademicPress,1985.

[6] R.G. Larson, *The Structure and Rheology ofComplex ;Fluids.* NewYork :Oxford University Press,1999.

[7] H. Rehage and H. Hofhnann. ·'Viscolastic surfactant solutions: u10del systems

For rheological research,"*Mol.Phy8..*vol.74,no.5,pp.933-973,1991.

[8] P. Schurtenberger, R. Scartazzini, L. Magid, M. Leser, and P. Luisi. "Structural and dynamic properties of polymer-liker everse micelles,"*J.Phys.Chern.,*vol.94,no.9,pp.3695-3701,1990.

[9] S. H. Tung, Y. E. Huang, and S. Ragharnn A new reverse wormlike micellar system: mixtures of bile salt and lecirltinin organic liquids,"*J.Arn.Chern.Soc.,*vol.128,pp.5751·--5756,2006.

[10] R. Laughlin, *The Aqueo us Phas eBehavior ofSurfactants.* NewYork:Academic Press,1994.

[11] J. Appell. G. Porte. A. Khatory. F. Kern, and S. Candau, "StatiC' and dynamic properties of a network of wormlike surfactant micelles (etylpyridinium chlorate in sodium chlorate brine),"*J.Phys.II,*vol.2,pp.1045--1052,1992.

[12] J.P. Rothstein,' transient extensional rheology of wormlike micelle solutions,"

*J01mialofRheology,*vol.47,no.5,pp.1227--1247,2003.

[13] A. Bhardwaj. E. Miller, and J.P. Rothstein, "Filament stretching and capillary breakup extensional rheometry measurements of viscoelastic wormlike micelle solutions," *Journal of Rheology,*vol.51,no.4,pp.693-719,2007.

[14] S. Chenand J.P. Rothstein, "Flow of a wormlike micelle solution past a falling sphere.''*Journal of Non-NewtonianFluidMechanics,*vol.11?,no.23,pp.205-234,2004.

[15].J.R. Gladdenand A.Belmonte. ·'Motion of a viscoelastic micellar fluid around a cylinder: Flow and fracture.''*Phys.Rev.Lett.,*vol.98,no.22,p.224501,2007.

[16]P. W. Bearman, "Vortex shedding from oscillating b luff bodies." *Annu. Rev.*

*Fl'(J,idMech.,*vol.16,110. 1.pp.195--222.1984.

[17]RD.Blevins. *Flow-inducer vibration* Krieger Pub.Co.,Malabar,Fla., 1990.

[18]MP. Paidonss is. S.J. Price, and E.de Langre. *Fluid- Structure Interactions-Cross-Flow-Induced Instabilities* .Cambridge University Press, NewYork, 2011,vol.1.

[19] M. P. Paidloussis. *Fluid- Structure Interactions: Slender Structures and Arial Flow. Vol.1.* San Diego, CA: Academic Press Inc.1998.

[20] M. Padoissis, *Fluid-Structcure Inter-actions :Slender Structures and Arial Flow, Vol.2.* Academic Press, London, 2004.

[21] C. William son and It Govardhan, ''Vortex-induced vibrations," *Amm. Rev.*

*Fluid Mech..*vol.6.pp.413--455.2004.

[22] T. Sarpkaya, "A critical review of the intrinsic nature of vortex-induced vibrations, "*J. Fluids and Structure..*vol. HJ.110. -L pp.389-447,2004.

[23] P. Bearman, ''Circular cylinder wakes and vortex-induced vibrations," *Journal of Fluids and Structures,*vol.27.llU. 56.pp.o-18...658,2011.

[24] A. Ougoren and D. Rockwell, "Flow structure from an oscillating cylinder part

1.mechanisms of phase shift and recovery in the near wake," *Journal ofFluid Mechanics* ,vol. 191,no.1,pp. 197-223.1988.

[25] J. Carberry.J.Sheridan, and D. Rockwell, "Controlled oscillations of a cylinder :forces and wake modes, '·*Journal of Ffoidl'vfechanics,*vol.538.pp.31--70,2005.

[26]J.S. Leontini. B.E. Stewart M.C. Thomp son, and K. Hourigan, "Wake state and energy transitions of an oscillating cylinder at lowreyn olds number,"*Physics ofFluids(1994-present).*vol.18.no.6,pp. .2006.

[27] T. Prasauth and S. Mittal. Vortex- induced l vibrations of a circular cylinder at loweryn olds numbers.''*Joiu.. nal of F foid Mechanics,* vol.594,p.463,2008.[28] D. Jeon and M. Gharib. "On circular cylinders under going two-degree-of-freedom forced motions. " Journal of fluids and Structures, Vol. 15 no. 3 pp 533-541 2001